Green tea extract assisted green synthesis of reduced graphene oxide: Application for highly sensitive electrochemical detection of sunset yellow in food products

Elham Vatandost[a], Azade Ghorbani-HasanSaraei[a], Fereshteh Chekin[b],*,
Shahram Naghizadeh Raeisi[a], Seyed-Ahmad Shahidi[a]

[a] Department of Food Science and Technology, Ayatollah Amoli Branch, Islamic Azad University, Amol, Iran
[b] Department of Chemistry, Ayatollah Amoli Branch, Islamic Azad University, Amol, Iran

ARTICLE INFO

ABSTRACT

The search to find simple, cost-effective, environmentally friendly method for synthesising of reduced graphene oxide (rGO) has motivated the use of various natural materials. Also, monitoring of sunset yellow (SY) level in foods due to the potential negative side effects is imperative. In this study, tea extract was explored as reducing and stabilizing agent for synthesising of rGO. The rGO modified carbon paste electrode (rGO/CPE) was used as a highly sensitive electrochemical sensor for the detection of SY. The rGO/CPE, due to the large surface area, showed strong enhancement effect on electrochemical oxidation of SY. Under optimized conditions, linear range between 0.05 and 10 μM with a detection limit of 27 nM could be achieved. The proposed sensor was used to determine the amount of SY in food products with satisfactory results, and the results were in good agreement with the results obtained by UV–Vis spectroscopy.

1. Introduction

Graphene, a carbon material with unique physicochemical features such as excellent electrical and thermal conductivity, high surface area and strong mechanical strength (Khan et al., 2015) has wide applications such as biosensors, biotechnologies, fuel cells, solar cells, energy storage, electronic, supercapacitor and biomedicine (Chen, Yan, Liu, & Niu, 2016; Farazas, Mavropoulos, Christofilos, Tsiaoussis, & Tsipas, 2018; Ojha, Saha, Kolevc, Kumar, & Ganguli, 2016; Zhang et al., 2015).

The synthesis of graphene which is one atomic thick sheet of carbon in large scale production, low cost and eco-friendly method is a big challenge today. An efficient method for synthesizing GO was improved by Hummers et al. (Calderón-Ayala et al., 2017; Chekin, Singh, et al. 2016; Chekin, Teodorescu, et al., 2016). The current synthesis methods are based on modifications and improvements of this method. In chemicals reduction method, reduction agents are used such as hydrazine, hydroquinone, sodium borohydride, and ascorbic acid (Chandu, Sriram Mosali, Mullamuri, & Bollikolla, 2017; Chekin, Singh, et al. 2016; Chekin, Teodorescu, et al., 2016; Kavinkumar, Varunkumar, & Sellaperumal Manivannan, 2017). However, despite several advantages, the chemical reductions are highly toxic in nature, hazardous, and harmful to environment and human life (Tran, Kabiri, & Losic,

2014) and synthesized rGO tends to agglomerate strongly due to interlayer attractive Vander Waals forces.

In environmentally friendly approach called biosynthesis or green synthesis and currently is the hottest topic in the graphene community, various natural materials such leaf extracts, peels, bio-compounds and microbes is used as reducing agent (Chandu et al., 2017; Chettri, Vendamani, Tripathi, Pathak, & Tiwari, 2016; Sathishkumar et al., 2016; Wang, Shi, & Yin, 2011; Wang, Yao, Shen, & Wang, 2016). Plant extracts are attractive alternatives because of easily available, comparatively cheap and environmental friendly (Navyatha, Kumar, & Nara, 2016).

Green tea contains high levels of polyphenols such as flavonoids, gallic acid and tannic acid, which may have a number of positive health effects in the prevention of lifestyle-related diseases (Alegria et al., 2018; Masek, Chrzescijanska, Latos, Zaborski, & Podsędek, 2017; Zhu et al., 2017). The important compounds in the plant extract are hydroxyl and carbonyl groups. Both functional groups allow plant extract to act as reducing agent as well as stabilizing agent (Lambri et al., 2015). The produced rGO sheets are functionalized by extract polyphenols.

Sunset yellow commercially used as additive in pharmaceuticals and cosmetics, with the advantages that it can be easily mixed to

---

* Corresponding author.
  E-mail address: f.chekin@iauamol.ac.ir (F. Chekin).

achieve ideal colours and because of its low price compared to the natural dyes (Qiu et al., 2016). The SY will be pathogenic when it is excessively consumed (Wang et al., 2016; Zhang, Liu, Zheng, Huang, & Wan, 2009). Therefore, it is important to detect SY with desired sensitivity and accuracy. The several methods were reported to ensure the control of SY level in foods such as electrochemical (Cheng, Xia, Tong, & Wu, 2015; Songyang, Yang, Xie, Hao, & Song, 2015; Tang, Wang, Liu, & Sun, 2016; Wang et al., 2016; Wang, Gao, Sun, & Zhao, 2014; Wang, Yang, Wang, Yang, & Du, 2015; Ya et al., 2017), chromatographic (Mahmoodi, Faraji, & Ziarat, 2016; Sulekova, Hudák, & Smrcova, 2016), spectrophotometric (Guray, 2018; Yuan et al., 2016; Zeynali & Manafi-Khoshmanesh, 2015; Zhu, Zhang, & Yang, 2015) and immunological methods (Li et al., 2013). Owing to the electroactive nature of SY and rapid response, cost effectiveness, eco-friendly, high sensitivity and easy operation of method, electrochemical methods were considered most attractive for SY analysis (Tang et al., 2016).

Due to health benefits and antioxidant properties, the use of green tea for the production of biocompatible rGO is being tested. Also, The quantitative determination at trace levels of synthetic dyes is currently an important analytical task, because of the need to eliminate possible exposure of consumers to over-dosage. In this work, we report an eco-friendly approach for the preparation of rGO using green tea extract as a reducing and stabilizing agent and investigate the performance of an electrochemical sensor, obtained by the deposition of rGO onto carbon paste electrode, for the detection of SY (Fig. 1). The proposed sensor offers a simple and fast way for SY sensing in food samples with a short analysis time, making the concept of interest.

2. Experimental

2.1. Materials

Sunset yellow (SY), Potassium hexacyanoferrate(II) ($[K_4Fe(CN)_6]$), potassium chloride (KCl), and phosphate buffer tablets (PBS, 0.1 M) were purchased from Sigma-Aldrich and used as received. Graphene oxide (GO) powder was purchased from Iranian Nanomaterials Pioneers. Food samples were prepared from local market (Amol, Iran).

2.2. Preparation of green tea extract

The green tea used in this work was bought from local market (Rasht, Iran). 2 gr weight of green tea was sonicated with 50 mL of distilled water at 50 °C for 30 min to obtain green tea extract. The extract was isolated by filtration and stored in fridge for using.

2.3. Preparation of reduced graphene oxide (rGO)

Reduced graphene oxide (rGO) was prepared from GO precursor using green tea extract. Briefly, green tea extract (10 mL) was added drop by drop for 45 min to 20 mL of GO aqueous suspension (0.5 mg/mL) and the mixture was refluxed for 6 h at 60 °C which the reduced GO gradually precipitated out the solution. The product was isolated by solution centrifugation at 15000 rpm for 15 min, washed with water for 4 times, and dried in an oven at 70 °C overnight.

2.4. Fabrication of rGO modified electrode

The carbon paste electrode (CPE) was prepared based on previous report (Nikkhah, Tahermansouri, & Chekin, 2018). The graphite powder plus paraffin hand-mixed until a uniformly wetted paste was obtained. Then the carbon paste was packed into a glass tube (with internal radius 3 mm). Electrical contact was made by a copper wire. The new surface of electrode was obtained by polishing it on a weighing paper.

Mg of rGO was added to 1 mL of water and sonicated for 30 min. 5 μL of this solution was drop-casted onto the CPE and allowed to dry in an oven at 50 °C.

2.5. Characterization

Electrochemical experiments were performed with potentiostat/galvanostat of Sama 500-c Electrochemical Analysis system, Sama, Iran and Metrohm Autolab, Netherlands. A conventional three-electrode system consisting of $Ag|AgCl|KCl_{3M}$ as the reference electrode, rGO/CPE or CPE as working electrode and a platinum wire as auxiliary electrode was used. UV–Vis spectra of samples were recorded by UV–Vis spectrophotometer (UV-1900, Shimadzu Co., Japan). FT-IR spectra of the GO and rGO were recorded by (IR Tracer-100, Shimadzu Co., Japan). The FE-SEM images were carried out by MIRATES-CAN-XMU (Czech Republic).

2.6. Analysis of food samples

500 μL or 1 mg of food samples was transferred to the electrochemical cell containing 10 mL PBS (0.1 M; pH = 4.00) and the oxidation current was measured by DPV. Also, the concentration of SY in samples was determined by UV–Vis spectroscopy at wavelength of 380 nm with diluting 500 μL or 0.5 mg of food sample in 5 mL water.
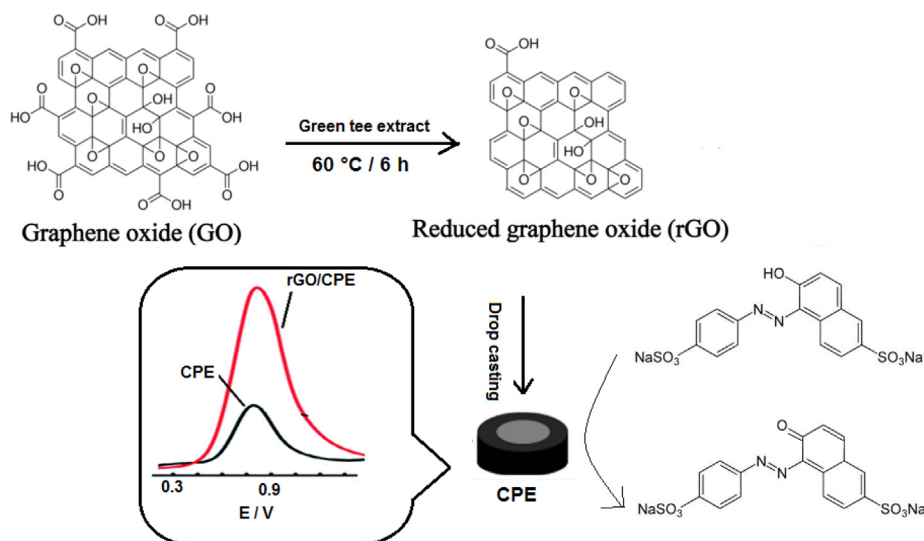

Fig. 1. Formation of rGO and schematic presentation of electrochemical sensor modified with rGO for the oxidation of sunset yellow.
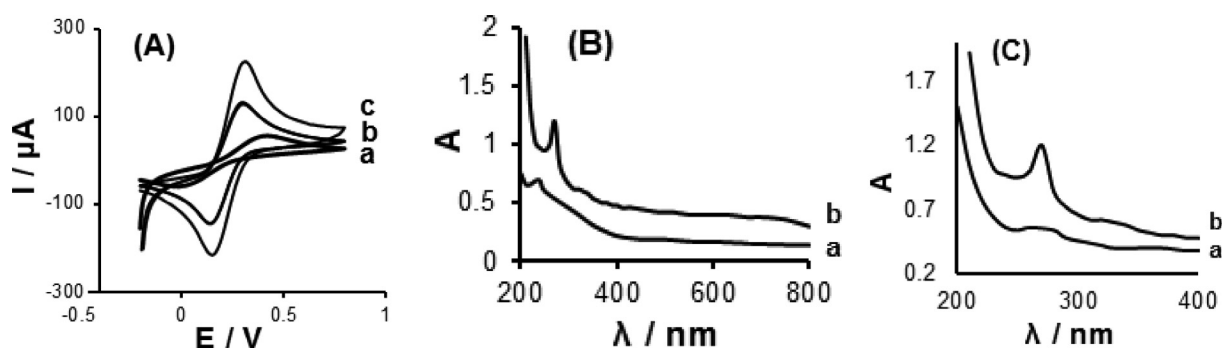
Fig. 2. (A) Cyclic voltammograms recorded on CPE (a), GO/CPE (b) and rGO/CPE (c) using $[Fe(CN)_6]^{4-}$ (5 mM)/PBS (0.1 M), scan rate = 100 mV s^{-1}; UV–Vis spectra of GO (a) and rGO (b) aqueous suspension (1 mg/mL); (C) UV–Vis spectra of rGO prepared with addition of 3 (a) and 10 mL green tea extract.

3. Results and discussions

3.1. Electrochemical test

Fig. 2 indicates the electrochemical behavior of CPE before and after modification by drop casting with GO and rGO. Fig. 2A shows the cyclic voltammetry of the different interfaces using $[Fe(CN)_6]^{3-/4-}$ as a redox couple. The redox current was increased considerably for rGO/CPE, being larger than those recorded for GO/CPE and CPE. The increased surface area together the good electronic properties of rGO, supporting rapid electron transfer, are mostly likely responsible for the current enhancement.

The real electrochemical active surface area of GO/CPE and rGO/CPE was determined by plotting the peak current as a function of the square root of the scan rate for $[Fe(CN)_6]^{4-}$ (5 mM). From the slopes of these graphs and using Eq. (1):

$$A = slope/(268.6 \times n^{3/2} \times D^{1/2} \times C) \tag{1}$$

where A is the electrochemical active surface area (cm^2), n the number of electrons transferred (n = 1), D the diffusion coefficient of $[Fe(CN)_6]^{4-}$ and C the concentration of $[Fe(CN)_6]^{4-}$. In contrast to GO/CPE with an active surface area of 0.09 cm^2, rGO/CPE shows an increased surface area (A = 0.18 cm^2). The higher electroactive area of rGO/CPE recommends rGO/CPE as an efficient platform for determination of many analytes.

3.2. UV–Vis spectroscopy

The reduction of GO was monitored by recording UV–Vis absorption spectra. As shown in Fig. 2B, the absorption peak of the GO suspension is around 240 nm, while the absorption peak of the reduced suspension shifts into wavelength of around 270 nm. This red shift value may be attributed to the deoxygenation of the GO suspension. Similar feature have been observed for the reduction of GO with phytomolecules reported in literatures (Calderón-Ayala et al., 2017; Fernández-Merino et al., 2010; Khan et al., 2015; Khanra et al., 2012).

The role of the green tea was confirmed as bio-reductant agent by UV–Vis spectroscopy. Fig. 2C shows UV–Vis absorption spectra of rGO suspension prepared with different value of green tea extract. As observed, the intensity of the absorption peak in around 270 nm is creased with high value of green tea extract. This was confirmed that the phytomolecules of green tea extract not only act as reducing agent but also functionalize surface of rGO sheets (Fernández-Merino et al., 2010; Wang et al., 2011).

3.3. SEM study

The surface morphology of samples was also evaluated by scanning electron microscope (SEM). Fig. 3 shows the SEM images of GO and synthesized rGO samples. The layers of GO (Fig. 3A) have a wavy shape,
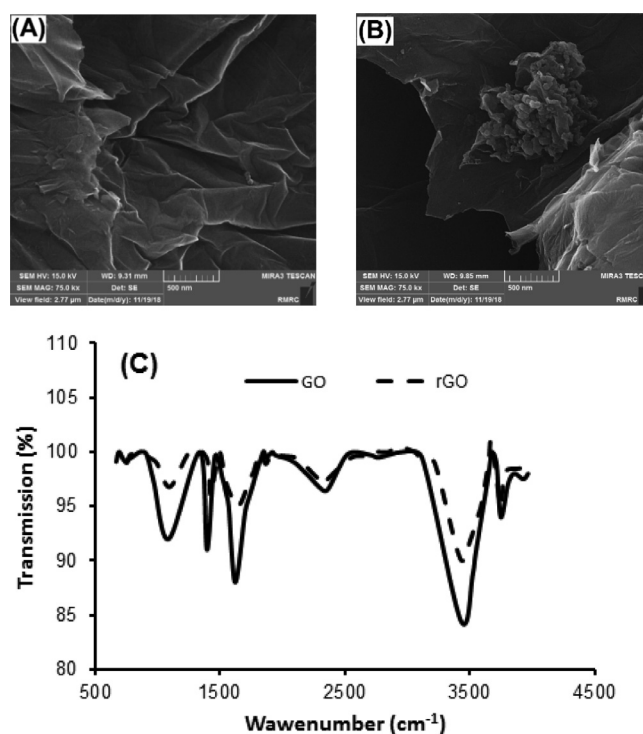

Fig. 3. SEM images of (A) GO and (B) rGO; (C) FT-IR spectra of GO and rGO.

sheet-like structure and thin layers, smooth surface and wrinkled edge. The image of rGO (Fig. 3B) clearly shows morphology with multi-layered sheets onto each other, a rougher surface and wave-shaped corrugated structures. Also, the sphere shape agglomerations are seen on rGO sheets. This observation is in good agreement with UV–Vis absorption spectra of rGO and confirms the formation of functionalized reduced graphene.

3.4. FT-IR analysis

Furthermore, the reduction of GO was also monitored using FT-IR analysis. The FT-IR spectra of GO and rGO are shown in Fig. 3C. The GO exhibits intense peaks. The decrease in the intensity of the bands like broad band at 3427 cm^{-1} belonging to the hydroxyl groups of GO and slight shifts are seen at same position such as the bands at ~ 3427, ~2340, ~1622, and ~1090 cm^{-1}. This confirms reduction of GO.

3.5. Electrochemical sensing of SY

Fig. 4A depicts the electrochemical behavior of bare CPE and CPE modified with GO and rGO towards the electrochemical response of
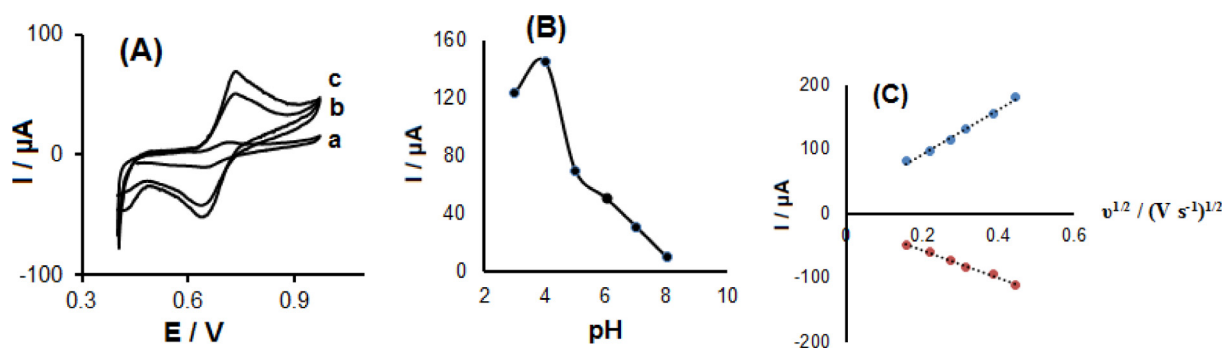
Fig. 4. (A) Cyclic voltammograms recorded of (a) CPE, (b) GO/CPE and (c) rGO/CPE in PBS (0.1 M, pH 4.00) containing SY (0.1 mM), scan rate = 100 mV s^{-1}; (B) Influence of pH on the SY anodic peak current; (C) Dependence of the scan rate on anodic and cathodic peak current.

0.1 mM sunset yellow in the 0.1 M PBS (pH 4.00). A bare CPE shows small oxidative and reduction currents at ~0.750 V and ~0.641 V, whereas anodic (E_{pa}) and cathodic (E_{pc}) peak potential of SY at rGO modified CPE are recorded at ~0.730 V and ~0.645 V with larger oxidation and reduction currents. The E_{pa} and E_{pc} are comparable to those reported using Au-Pd and reduced graphene oxide (rGO) nanocomposite modified glassy carbon electrode in pH 4.00 (E_{pa} = 0.753 V and E_{pc} = 0.705 V), Au-rGO modified glassy carbon electrode in pH 4.00 (E_{pa} = 0.752 V and E_{pc} = 0.688 V), multi-walled carbon nanotubes modified glassy carbon electrode in pH 8.00 (E_{pa} = 0.630 V and E_{pc} = 0.600 V), poly L-cysteine modified glassy carbon electrode in pH 2.50 (E_{pa} = 0.858 V and E_{pc} = 0.772 V), Ag modified glassy carbon electrode in pH 2.50 (E_{pa} = 0.862 V and E_{pc} = 0.778 V), Ag and poly L-cysteine modified glassy carbon electrode in pH 2.50 (E_{pa} = 0.868 V and E_{pc} = 0.772 V), Ag and polypyrrole decorated oxidized single-walled carbon nanotubes modified glassy carbon electrode in pH 7.00 (E_{pa} = 0.673 V and E_{pc} = 0.633 V) and zinc oxide nanoflower modified carbon paste electrode in pH 5.00 (E_{pa} = 0.756 V and E_{pc} = 0.718 V), (Tang et al., 2016; Wang et al., 2014, 2016; Ya et al., 2017; Zhang et al., 2009). The highest oxidation and reduction currents are however detected on rGO/CPE (~7 times in comparison with CPE), indicating that the rGO nanosheets functionalized with phytomolecules have been successfully attached to the surface of CPE and formed a tunable kinetic barrier toward SY electrochemical response. The π-π stacking interaction as well as electrostatic interactions between the aromatic components of SY and rGO prevailing the origin of this behavior.

Indeed, the effect of pH on the electrochemical behavior of SY on rGO/CPE showed that the oxidation peak current increased from 3.00 to 4.00 and reached the maximum value at pH 4.00, then decreased with the deformation of the curves (Fig. 4B). To evaluate the behavior of SY oxidation, the anodic peak potential, E_{pa}, was plotted versus the solution pH. The results demonstrated a plot with a linear regression of E_{pa} = 2.54–51.84 × pH (R = 0.992), indicating an electrode process with exchanged number of protons and electrons being the same (Qiu et al., 2016; Rovina, Siddiquee, & Shaarani, 2016) according to Scheme 1. The influence of scan rate on the electrochemical response of SY was also investigated. The anodic and cathodic peak currents were showed linearly proportional to square root of the scan rate (Fig. 4C), suggesting that the reaction is a diffusion-controlled process.

3.6. Validation of the proposed method

The electrocatalytic response of bare CPE and CP electrodes
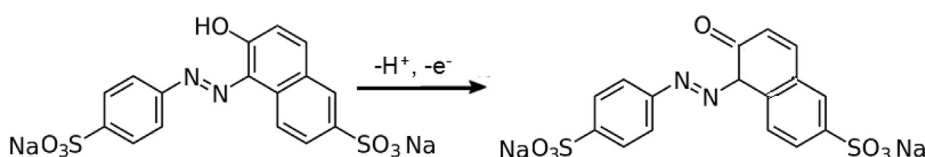
modified with GO and rGO was also investigated toward the electrochemical oxidation of 10 μM SY in the 0.1 M PBS (pH 4.00) by differential pulse voltammetry (DPV). As shown in Fig. 5A, the oxidation peak of SY at rGO/CPE has highest current, indicating that the rGO nanosheets has significantly improved performance toward SY oxidation. The unique surface chemistry of rGO interface allows π–π stacking interactions with SY. To determine whether the rGO/CPE sensor can be applied for detection of SY, the oxidation peak current of SY was measured upon addition of increasing concentrations of SY using DPV (Fig. 5B). The linear relationship between the oxidative peak current and the concentration of SY in the range of 0.05–10 μM was recorded with a correlation coefficient of 0.9923 according to I (μA) = 2.353 [SY] (μM) + 12.853 (Inset of Fig. 5B). The detection limit (LOD) of SY was found to be 27 nM according to following equation:

$$LOD = 3S_b/m \tag{2}$$

where S_b is the standard deviation of the blank and m is the slope of the calibration curve. The LOD and linear rang (LDR) are comparable to (Table 1) that reported by Zhang et al using MWCNT modified glassy carbon electrode (MWCNT/GCE), Au-Pd-rGO modified glassy carbon electrode (Au-Pd-rGO/GCE), Au nanoparticles modified carbon paste electrode (AuNP/CPE), graphene nanoplatelet modified carbon-–ceramic electrode (G/CCE) and carbon nanotube-ionic liquid modified carbon–ceramic electrode (CN-IL/CCE) (Ghoreishi, Behpour, & Golestaneh, 2012; Majidi, Fadakar Bajeh Baj, & Naseri, 2012; Majidi, Pournaghi-Azar, Fadakar Bajeh Baj, & Naseri, 2014; Wang et al., 2016; Zhang et al., 2009). The ease and one step procedure of making rGO/CPE sensor and the markedly high sensitivity (2328 μA mM^{-1}) of sensor might be however an advantage when it comes for sensing in food products.

The reproducibility of the four electrode fabrication to sense SY is expressed in term of relative standard deviation, which is found to be 5.7% at a SY concentration of 1 μM. The repeatability of the sensor response was evaluated by performing four determinations using a single sensor with the same SY solution (1 μM). The RSD for these determinations was found to be 7.1%. Regeneration of the electrode could be achieved upon immersion of the sensor in NaOH-H$_3$PO$_4$ (pH = 12.0) solution for 30 min. The long-term stability of the sensor was in addition evaluated, showing a loss of 8% when tested in 5 μM SY solution after stored at 4 °C for 15 days.

The influence of various foreign species such as glucose (Glu), ascorbic acid (AA), oxalic acid (OA), citric acid (CA), Ca^{+2}, K$^+$, Na$^+$, Fe^{+3}, Zn^{+2}, tartrazine (Tar), allura red (All) and amaranth (Ama) in the

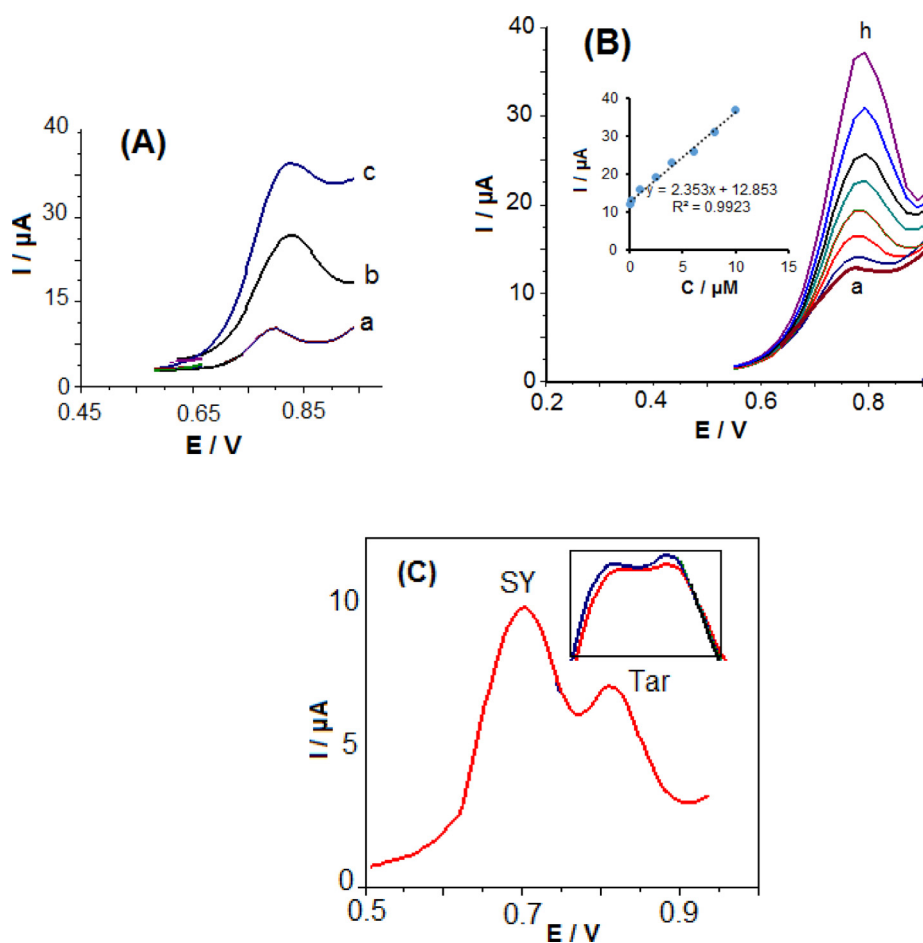**Scheme 1.** Proposed electrochemical oxidation of SY.

Fig. 5. (A) Differential pulse voltammograms recorded of (a) CPE, (b) GO/CPE and rGO/CPE in PBS (0.1 M, pH 4.00) containing SY (10 μM). (B) Differential pulse voltammograms of rGO/CPE sensor in PBS (0.1 M, pH 4.00) upon the addition (a) 0.05, (b) 0.1, (c) 1, (d) 2, (e) 4 (f) 6, (g) 8 and (h) 10 μM of SY. Inset: Change of oxidation peak current as a function of SY concertation; (C) DPV of a solution containing Tar and SY (0.1 mM each) in PBS (0.1 M, pH 4.00); Inset: DPV of a solution containing SY + Ama (black curve) and SY + All (red curve).

Table 1
Analytical parameters for voltammetric determination of SY at different modified electrodes.

Electrode	Linear range (μM)	LOD (nM)	Ref
MWCNT/GCE	0.05–11	22	Zhang et al. (2009))
Au-Pd-rGO/GCE	0.7–332	1.5	Wang et al. (2016)
AuNP/CPE	0.1–2	30	Ghoreishi et al. (2012)
G/CCE	0.1–15	73	Majidi et al. (2014)
CN-IL/CCE	0.1–110	100	Majidi et al. (2012)
rGO/CPE	0.05–10	27	This work

Table 2
Determination and recovery of SY in food samples.

Food sample	Added (μM)	Found (μM)	Recovery %	UV–Vis (μM)	t_{exp}	F_{exp}
Fanta	–	4.5	–	4.7	2.35	4.97
	10	14.7	102 ± 1.1	14.5		
Mirinda	–	5.2	–	5.5	1.93	5.16
	10	14.8	96 ± 2.8	15.1		
Cheese snack	–	8.9	–	8.4	2.29	3.34
	10	19.4	105 ± 3.4	19.1		
Cheetoz	–	10.2	–	9.6	2.41	4.27
	10	19.8	96 ± 1.9	20.3		

Theoretical values for t = 2.31 and F = 5.79 (p = 0.05).

determination of SY was investigated using DPV when presents at equal concentration with SY. The results showed that amaranth slightly interferes, whereas allura red interferes in determination of SY. The other species did not show interference (Fig. 5C), showing excellent selectivity.

3.7. Sunset yellow sensing in food samples

To finally see the feasibility of the developed SY sensor for the analysis, 4 food samples (Fanta, Miranda, Snack, and Chitoz) were tested (Table 2). The SY concentrations were detected several order of magnitude lower in the case of Fanta and Miranda when compared to Snack, and Chitoz. The results of proposed method were compared to those recorded with a reference method (UV–Vis spectroscopy) using Student's *t*-test for accuracy and F-test for precision. The results listed in Table 2 revealed the proposed method does not significantly differ in precision and accuracy from the reference method and the rGO/CPE sensor is well adapted for SY detection in food samples. The validity and accuracy of the proposed method was also carried out by recovery

testing using the standard addition method. Known amount of the pure SY was added to food products. The obtained mean recoveries (96, 102 and 105%) and relative standard deviations (1.1, 1.9, 2.8 and 3.4%) suggest good accuracy of the proposed method.

4. Conclusions

A new rGO has been synthesized via facile and environmentally friendly process. The SEM, FT-IR and UV–Vis spectroscopy results confirmed the synthesis of rGO. The observed higher current for the oxidation and reduction of SY on rGO/CPE points to its electro-catalytic activity towards SY oxidation and reduction. The rGO/CPE shows high sensitivity with LOD of 27 nM towards SY oxidation. This sensor with high electrical conductivity and the excellent catalytic activity provides good stability of the sensor. Additionally, rGO exhibited good performance for the determination of SY in food samples, suggesting that the

proposed method might be reliable and effective for SY sensing in real samples.

Declaration of Competing Interest

The authors declare that they have no known competing financial interests or personal relationships that could have appeared to influence the work reported in this paper.

Acknowledgment

References

Alegria, E. C. B. A., Ribeiro, A. P. C., Mendes, M., Ferraria, A. M., Botelho do Rego, A. M., & Pombeiro, A. J. L. (2018). Effect of phenolic compounds on the synthesis of gold nanoparticles and its catalytic activity in the reduction of nitro compounds. *Nanomaterials, 8*, 320–337.

Calderón-Ayala, G., Cortez-Valadez, M., Mani-Gonzalez, P. G., Britto Hurtado, R., Contreras-Rascón, J. I., Carrillo-Torres, R. C., ... Flores-Acosta, M. (2017). Green synthesis of reduced graphene oxide using ball milling. *Carbon Letters, 21*, 93–97.

Chandu, B., Sriram Mosali, V. S., Mullamuri, B., & Bollikolla, H. B. (2017). A facile green reduction of graphene oxide using Annona squamosa leaf extract. *Carbon Letters, 21*, 74–80.

Chekin, F., Singh, S. K., Vasilescu, A., Dhavale, V. M., Kurungot, S., Boukherroub, R., & Szunerits, S. (2016). Reduced graphene oxide modified electrodes for sensitive sensing of gliadin in food samples. *ACS Sensors, 1*, 1462–1470.

Chekin, F., Teodorescu, F., Coffinier, Y., Pan, G. H., Barras, A., Boukherroub, R., & Szunerits, S. (2016). MoS2/reduced graphene oxide as active hybrid material for the electrochemical detection of folic acid in human serum. *Biosensors and Bioelectronics, 85*, 807–813.

Chen, Zh., Yan, H., Liu, T., & Niu, S. (2016). Nanosheets of MoS$_2$ and reduced graphene oxide as hybrid fillers improved the mechanical and tribological properties of bismaleimide composites. *Composites Science and Technology, 125*, 47–54.

Cheng, Q., Xia, S., Tong, J., & Wu, K. (2015). Highly sensitive electrochemical sensing platforms for food colourants based on the property tuning of porous carbon. *Analytica Chimica Acta, 887*, 75–81.

Chettri, P., Vendamani, V. S., Tripathi, A., Pathak, A. P., & Tiwari, A. (2016). Self assembly of functionalised graphene nanostructures by one step reduction of graphene oxide using aqueous extract of Artemisia Vulgaris. *Applied Surface Science, 362*, 221–229.

Farazas, A., Mavropoulos, A., Christofilos, D., Tsiaoussis, I., & Tsipas, D. (2018). Ultrasound Assisted Green Synthesis and Characterization of Graphene Oxide. *International Journal of Nanoscience and Nanotechnology, 14*, 11–17.

Fernández-Merino, M. J., Guardia, L., Paredes, J. L., Villar-Rodil, S., Fernández, P. S., Martínez-Alonso, A., & Tascón, J. M. D. (2010). Vitamin C as an innocuous and safe reductant for the preparation of graphene suspensions from graphite oxide. *Journal of Physical Chemistry C, 114*, 6426–6432.

Ghoreishi, S. M., Behpour, M., & Golestaneh, M. (2012). Simultaneous determination of Sunset yellow and Tartrazine in soft drinks using gold nanoparticles carbon paste electrode. *Food Chemistry, 132*, 637–641.

Guray, T. (2018). Spectrophotometric determination of Sunset Yellow (E-110) in powdered beverages and pharmaceutical preparations after cloud point extraction method. *Journal of the Turkish Chemical Society, 5*, 479–492.

Kavinkumar, T., Varunkumar, K., & Sellaperumal Manivannan, V. R. (2017). Anticancer activity of graphene oxide-reduced graphene oxide-silver nanoparticle composites. *Journal of Colloid and Interface Science, 505*, 1125–1133.

Khan, M., Al-Marri, A. H., Khan, M., Shaik, M. R., Mohri, N., Farooq Adil, S., ... Siddiqui, M. R. H. (2015). Green approach for the effective reduction of graphene oxide using Salvadora persica L. Root (Miswak) extract. *Nanoscale Research Letters, 10*, 281–289.

Khanra, P., Kuila, T., Kim, N. H., Bae, S. H., Yu, D. S., & Lee, J. H. (2012). Simultaneous bio-functionalization and reduction of graphene oxide by baker's yeast. *Chemical Engineering Journal, 183*, 526–533.

Lambri, M., Torchio, F., Colangelo, D., Segade, S. R., Giacosa, S., De Faveri, D. M., & Rolle, L. (2015). Influence of different berry thermal treatment conditions, grape anthocyanin profile, and skin hardness on the extraction of anthocyanin compounds in the colored grape juice production. *Food Research International, 77*, 584–590.

Li, Z., Song, S., Xu, L., Kuang, H., Guo, S., & Xu, C. (2013). Development of an ultra-sensitive immunoassay for detecting tartrazine. *Sensors, 13*, 8155–8169.

Mahmoodi, N., Faraji, M., & Ziarat, P. (2016). Simultaneous determination of sunset yellow and carmoisine in orange flavored soft drink samples by high-performance liquid chromatography. *Journal of Applied Chemistry, 9*, 79–83.

Majidi, M. R., Fadakar Bajeh Baj, R., & Naseri, A. (2012). Carbon nanotube-ionic liquid (CNT–IL) nanocomposite modified sol-gel derived carbon-ceramic electrode for simultaneous determination of sunset yellow and tartrazine in food samples. *Food Analytical Methods, 6*, 1388–1397.

Majidi, M. R., Pournaghi-Azar, M. H., Fadakar Bajeh Baj, R., & Naseri, A. (2014). Formation of graphene nanoplatelet-like structures on carbon–ceramic electrode surface application for simultaneous determination of sunset yellow and tartrazine in some food samples. *Ionics, 21*, 863–875.

Masek, A., Chrzescijanska, E., Latos, M., Zaborski, M., & Podsędek, A. (2017). Antioxidant and antiradical properties of green Tea extract compounds. *International Journal of Electrochemical Science, 12*, 6600–6610.

Navyatha, B., Kumar, R., & Nara, S. (2016). A facile method for synthesis of gold nanotubes and their toxicity assessment. *Journal of Environmental Chemical Engineering, 4*, 924–931.

Nikkhah, Sh., Tahermansouri, H., & Chekin, F. (2018). Synthesis, characterization, and electrochemical properties of the modified graphene oxide with 4,40-methylenedianiline. *Materials Letters, 211*, 323–327.

Ojha, K., Saha, S., Kolevc, H., Kumar, B., & Ganguli, A. K. (2016). Composites of graphene-Mo$_2$C rods: Highly active and stable electrocatalyst for hydrogen evolution reaction. *Electrochimica Acta, 193*, 268–274.

Qiu, X., Lu, L., Leng, J., Yu, Y., Wang, W., Jiang, M., & Bai, L. (2016). An enhanced electrochemical platform based on graphene oxide and multi-walled carbon nanotubes nanocomposite for sensitive determination of Sunset Yellow and Tartrazine. *Food Chemistry, 190*, 889–895.

Rovina, K., Siddiquee, S., & Shaarani, S. M. (2016). Highly sensitive determination of sunset yellow FCF (E110) in food products based on Chitosan/Nanoparticles/MWCNTs with modified gold electrode. *Earth and Environmental Science, 36*, 012023–012029.

Sathishkumar, G., Pradeep, K. J., Vignesh, V., Rajkuberan, C., Jeyaraj, M., Selvakumar, M., ... Sivaramakrishnan, S. (2016). Cannonball fruit (Couroupita guianensis, Aubl.) extract mediated synthesis of gold nanoparticles and evaluation of its antioxidant activity. *Journal of Molecular Liquids, 215*, 229–236.

Songyang, Y., Yang, X., Xie, S., Hao, H., & Song, J. (2015). Highly-sensitive and rapid determination of sunset yellow using functionalized montmorillonite-modified electrode. *Food Chemistry, 173*, 640–644.

Sulekova, M., Hudák, A., & Smrcova, M. (2016). The determination of food dyes in vitamins by RP-HPLC. *Molecules, 21*, 1368–1375.

Tang, Y., Wang, Y., Liu, G., & Sun, D. (2016). Determination of sunset yellow and tartrazine using silver and poly (L-cysteine) composite film modified glassy carbon electrode. *Indian Journal of Chemistry, 55*, 298–303.

Tran, D. N., Kabiri, S., & Losic, D. A. (2014). Green approach for the reduction of graphene oxide nanosheets using non-aromatic amino acids. *Carbon, 76*, 193–202.

Wang, J., Yang, B., Zhang, K., Bin, D., Shiraishi, Y., Yang, P., & Du, Y. (2016). Highly sensitive electrochemical determination of Sunset Yellow based on the ultrafine Au-Pd and reduced graphene oxide nanocomposites. *Journal of Colloid and Interface Science, 481*, 229–235.

Wang, J., Yang, B., Wang, H., Yang, P., & Du, Y. (2015). Highly sensitive electrochemical determination of sunset yellow based on gold nanoparticles/graphene electrode. *Analytica Chimica Acta, 893*, 41–48.

Wang, M., Gao, Y., Sun, Q., & Zhao, J. (2014). Sensitively simultaneous determination of sunset yellow and tartrazine in foods based on polypyrrole modified oxidized single-walled carbon nanotubes. *Journal of The Electrochemical Society, 161*, B297–B304.

Wang, R., Yao, Y., Shen, M., & Wang, X. (2016). Green synthesis of Au@Ag nanostructures through a seed-mediated method and their application in SERS. *Colloids and Surfaces A: Physicochemical and Engineering Aspects, 492*, 263–272.

Wang, Y., Shi, X., & Yin, J. (2011). Facile synthesis of soluble graphene via a green reduction of graphene oxide in tea Solution and its biocomposites. *ACS Applied Materials and Interfaces, 3*(4), 1127–1133.

Ya, Y., Jiang, C., Li, T., Liao, J., Fan, Y., Wei, Y., ... Xie, L. (2017). A zinc oxide nanoflower-based electrochemical sensor for trace detection of Sunset Yellow. *Sensors, 17*, 545.

Yuan, Y., Zhao, X., Qiao, M., Zhu, J., Liu, S., Yang, J., & Hu, X. (2016). Determination of sunset yellow in soft drinks based on fluorescence quenching of carbondots. *Spectrochimica Acta A, 167*, 106–110.

Zeynali, K. A., & Manafi-Khoshmanesh, S. (2015). Simultaneous spectrophotometric determination of sunset yellow and quinolone yellow in a single step. *Journal of the Chinese Chemical Society, 62*, 772–779.

Zhang, J., Zhao, L., Liua, A., Li, X., Wu, H., & Lu, C. (2015). Three-dimensional MoS$_2$/rGO hydrogel with extremely high double-layer capacitance as active catalyst for hydrogen evolution reaction. *Electrochimica Acta, 182*, 652–658.

Zhang, W., Liu, T., Zheng, X., Huang, W., & Wan, Ch. (2009). Surface-enhanced oxidation and detection of Sunset Yellow and Tartrazine using multi-walled carbon nanotubes film-modified electrode. *Colloids and Surfaces B: Biointerfaces, 74*, 28–31.

Zhu, X., Xu, X., Liu, F., Jin, J., Liu, L., Zhi, Y., ... Yu, J. (2017). Green synthesis of graphene nanosheets and their in vitro cytotoxicity against human prostate cancer (DU 145) cell lines. *Nanomaterials and Nanotechnology, 7*, 1–7.

Zhu, Y., Zhang, L., & Yang, L. (2015). Designing of the functional paper-based surface-enhanced raman spectroscopy substrates for colorants detection. *Materials Research Bulletin Journal, 63*, 199–204.